JOC The Journal of Organic Chemistry

Article

pubs.acs.org/joc

Influence of Chlorine Substitution on the Hydrolytic Stability of Biaryl Ether Nucleoside Adducts Produced by Phenolic Toxins

Michael S. Kuska,[†] Mohadeseh Majdi Yazdi,[‡] Aaron A. Witham,[†] Heidi A. Dahlmann,[§] Shana J. Sturla,*[,§] Stacey D. Wetmore,*[,‡] and Richard A. Manderville*[,†]

[†]Departments of Chemistry and Toxicology, University of Guelph, Guelph, Ontario, N1G 2W1, Canada

[‡]Department of Chemistry and Biochemistry, University of Lethbridge, Lethbridge, Alberta, T1K 3M4, Canada

[§]Institute of Food, Nutrition and Health, ETH Zürich, 8006 Zürich, Switzerland

Supporting Information

ABSTRACT: A kinetic study is reported for the acid-catalyzed hydrolysis of oxygen (*O*)-linked biaryl ether 8-2′-deoxyguanosine (dG) adducts produced by phenolic toxins following metabolism into phenoxyl radical intermediates. Strikingly, the reaction rate of hydrolysis at pH 1 decreases as electron-withdrawing chlorine (Cl) substituents are added to the phenoxyl ring. The Hammett plot for hydrolysis at pH 1 shows a linear negative slope with ρ_X = −0.65, implying that increased Cl-substitution diminishes the rate of hydrolysis by lowering N^7 basicity. Spectrophotometric titration provided an N^7H^+ pK_a value of 1.1 for the unsubstituted adduct 8-phenoxy-dG (Ph-O-dG). Model pyridine compounds suggest N^7H^+ pK_a values of 0.92 and 0.37 for 4-Cl-Ph-O-dG and 2,6-dichloro-Ph-O-dG (DCP-O-dG), respectively. Density functional theory (DFT) calculations also highlight the ability of the 8-phenoxy substituent to lower N^7 basicity and predict a preference for N^3-protonation for highly chlorinated *O*-linked 8-dG adducts in water. The calculations also provide a rationale for the hydrolytic reactivity of *O*-linked 8-dG adducts in the gas-phase, as determined using electrospray mass spectrometry (ESI-MS). The inclusion of our data now establishes that the order of hydrolytic reactivity at neutral pH for bulky 8-dG adducts is *N*-linked > *C*-linked > *O*-linked, which correlates with their relative ease of N^7-protonation.

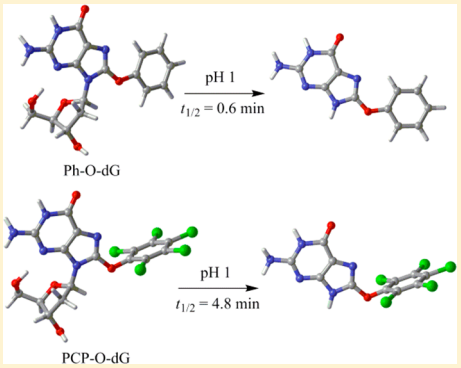

INTRODUCTION

The chemistry of DNA damage is diverse and complex. DNA is not indefinitely stable, and numerous sources of DNA-damaging agents of endogenous and exogenous origin can contribute further to its instability.[1] Depurination, the cleavage of the 1′-N^9 glycosidic bond between a purine base and its deoxyribose sugar, to afford abasic sites is a common type of damage suffered by genomic DNA.[2] Abasic sites are produced by exposure of DNA to oxidative stress, radiation, anticancer drugs, and mutagens, and if left unrepaired, abasic sites are mutagenic and cytotoxic.[3]

For unmodified 2′-deoxyguanosine (dG), exposure to acid accelerates the rate of depurination.[4] The acid-catalyzed hydrolysis of dG (Figure 1) is known to proceed via a stepwise mechanism.[5−7] The first step involves protonation at N^7, defined by the acid dissociation constant K_{a1}; the pK_{a1} value for N^7H^+-dG is 2.34.[8] The second step is rate-limiting and involves unimolecular cleavage of the glycosidic bond, defined by the rate constant k_1, to release protonated guanine as a good leaving group. Following cleavage, the oxocarbenium ion undergoes hydration to form the 1′-hydroxylated sugar. In duplex DNA, the corresponding tautomeric aldehyde has the potential to generate an interstrand DNA cross-link.[9]

Covalent modification of dG can also accelerate the rate of depurination to afford abasic sites. In duplex DNA the N^7 position of guanine is the most nucleophilic site and is particularly susceptible to attack by numerous alkylating agents.[10] The resulting N^7-guanine adduct contains a formal positive charge on the guanine ring, and is a good leaving group for depurination. Interestingly, the 8-site of dG is also susceptible to covalent modification by numerous electrophiles. Depending on the nature of the 8-substituent, the 8-guanine adduct can be an excellent leaving group for the depurination process. For example, reactive nitrogen species can generate the 8-NO_2-dG adduct that has been detected in the peripheral lymphocyte of humans exposed to cigarette smoke.[11] The 8-NO_2-dG lesion is unstable and depurinates at neutral pH by releasing 8-NO_2-G with a half-life ranging from 20 to 31 h in oligonucleotides.[12] In general, attachment of electron-withdrawing substituents to the 8-position of dG increases the rate of depurination through stabilization of the developing negative charge at N^9 during rate-limiting cleavage of the glycosyl bond.[13,14]

Received: May 22, 2013
Published: July 2, 2013

   dx.doi.org/10.1021/jo401122j | J. Org. Chem. 2013, 78, 7176−7185

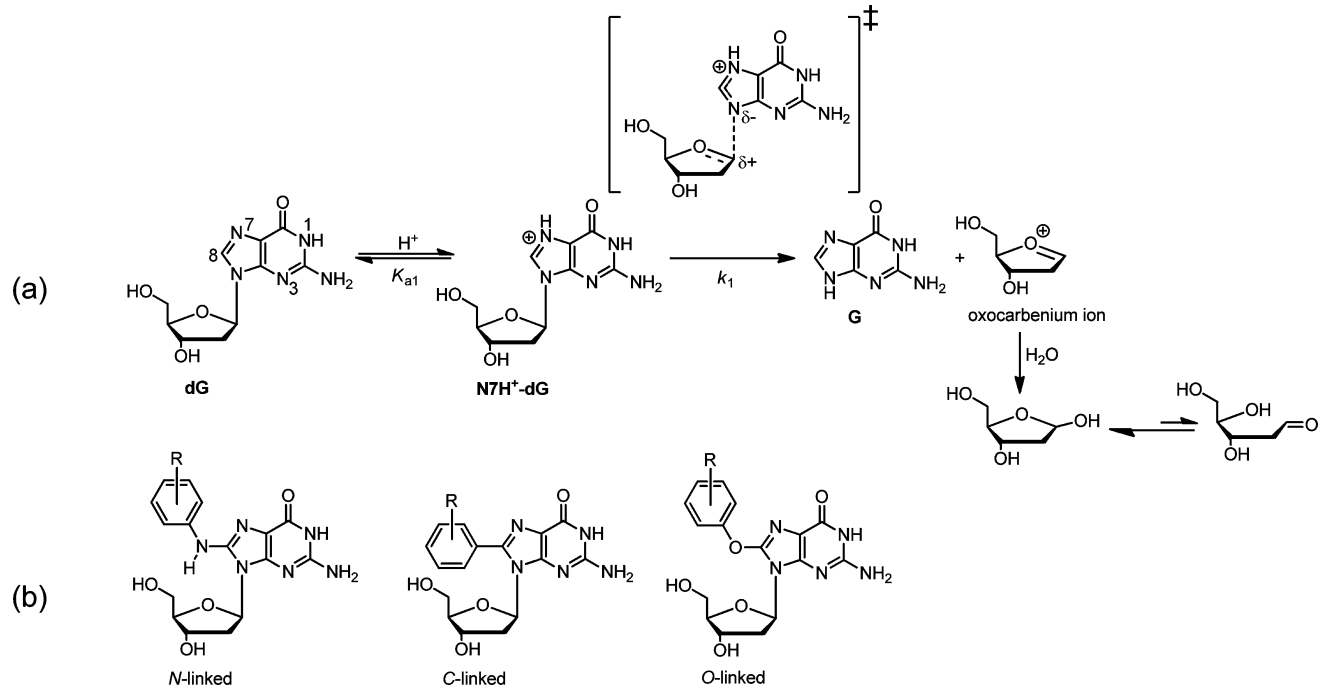

Figure 1. (a) Acid-catalyzed hydrolysis of dG. (b) Structures of *N*-linked, *C*-linked, and *O*-linked 8-dG adducts.

Scheme 1. Synthesis of Biaryl Ether Adducts

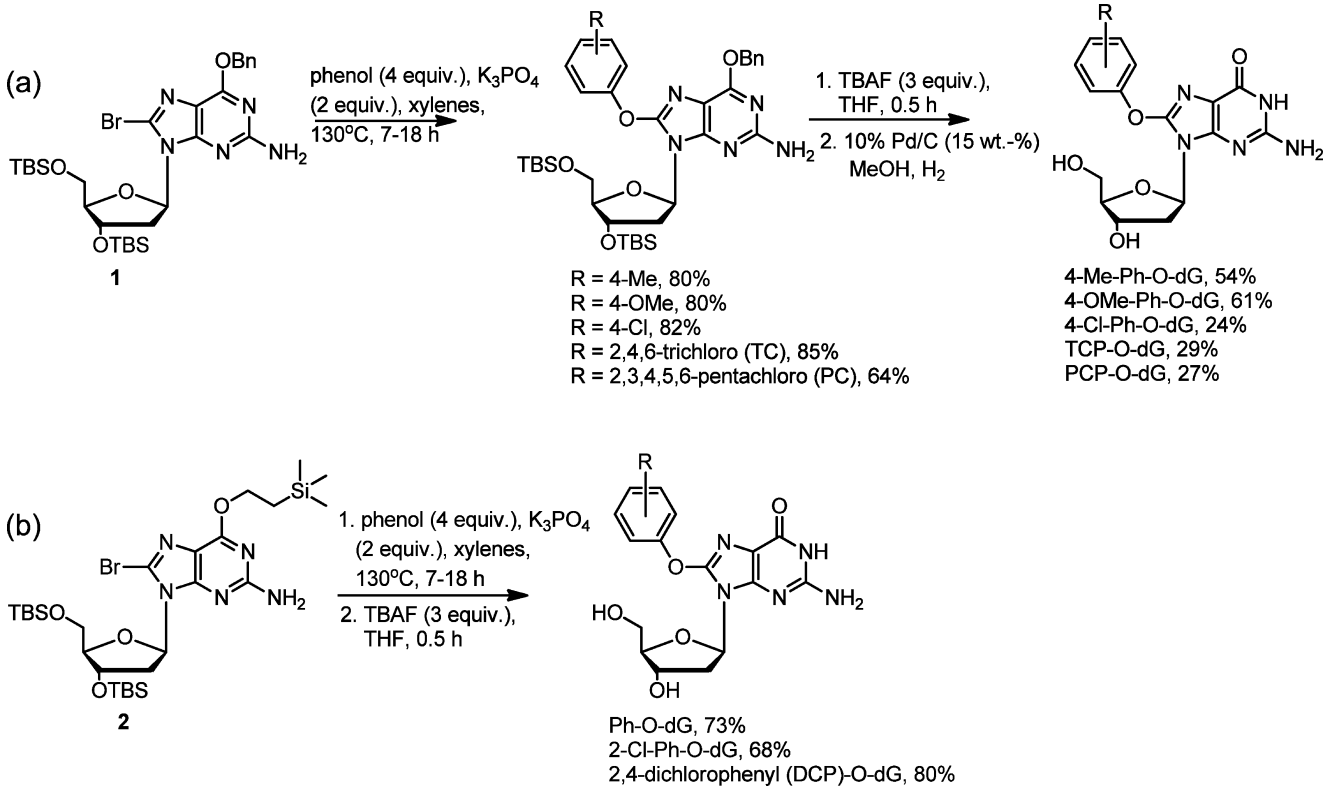

Bulky aryl ring systems also attach to the 8-site of dG to generate nitrogen-, carbon-, or oxygen-linked adducts (i.e., Figure 1b). The *N*-linked 8-dG adducts are the most common lesions produced from reactions of DNA with nitrenium ion metabolites from arylamine carcinogens.[15−17] The *N*-linked 8-dG adducts can undergo depurination under mildly acidic to neutral conditions where dG shows little reactivity.[18] In this case, the 8-arylamino substituent is electron-donating and increases pK_{a1} of the N^7H^+ nucleoside adduct by ∼2 pK_a units compared to unmodified N^7H^+-dG. Under acidic conditions (pH < 2), the *N*-linked 8-dG adducts are only 2- to 5-fold more reactive than dG, but between pH 3−6 the hydrolysis rates are accelerated by 40- to 1300-fold.[18] The rate increase is ascribed to the decrease in ionization constant of the *N*-linked N^7H^+-dG

dx.doi.org/10.1021/jo401122j | J. Org. Chem. 2013, 78, 7176−7185

adduct coupled with the release of steric strain upon removal of the sugar moiety.

The corresponding *C*-linked adducts[19] are produced by a range of chemical mutagens that include phenols,[20−22] polycyclic aromatic hydrocarbons (PAHs),[23] arylhydrazines,[24] estrogens[25] and nitroaromatics.[26] In this case, direct attachment of the aryl ring to afford the *C*-linked adduct has little impact on pK_{a1}.[19] However, in 0.1 M HCl (pH ∼ 1) the adducts are 5- to 45-fold more reactive than dG, which increases to 9- to 200-fold at pH 4.[19] Electron-withdrawing substituents at the *para*-position of the attached phenyl ring caused the greatest increase in hydrolysis rate relative to dG. Relief of steric strain upon removal of the deoxyribose sugar moiety coupled with stabilization of the developing negative charge at N^9 by electron-withdrawing *para*-substituents provided a rationale for the relative depurination efficiencies of *C*-linked 8-dG adducts.[19]

Finally, *O*-linked 8-dG adducts have been observed following metabolism of phenols by peroxidase enzymes in vitro.[27−29] Increased chlorination of the phenol ring favors *O*-linked adduct formation by increasing electrophilicity of the phenolic radical intermediate and decreasing the rate of bimolecular phenolic radical coupling.[28] Given that attachment of electron-withdrawing groups to the 8-position of dG can increase rates of hydrolysis to afford abasic sites,[13,14] we were particularly interested in establishing the hydrolytic stability of *O*-linked phenolic 8-dG adducts. Adducts bearing electron-deficient polychlorinated phenoxyl ring systems were expected to have enhanced susceptibility to hydrolysis. In this paper we present a kinetic and computational study of the hydrolysis of *O*-linked 8-dG adducts and draw comparison to hydrolysis rates already established for dG[5−7] and the corresponding *C*- and *N*-linked 8-dG adducts.[18,19]

RESULTS AND DISCUSSION

Synthesis of *O*-Linked 8-dG Adducts. A general method for the synthesis of *O*-linked 8-dG adducts has been developed by Dahlmann and Sturla.[30] As outlined in Scheme 1a, the synthesis involves base-promoted reactions of phenols with the protected 8-Br-dG analogue **1** in xylenes at 135 °C followed by TBAF-mediated desilylation of the 3′- and 5′-hydroxyls and catalytic hydrogenation to remove the O^6-benzyl (Bn) protecting group. *O*-Linked adducts 4-Me-Ph-OdG, 4-OMe-Ph-O-dG, 2,4,6-trichlorophenyl (TCP)-O-dG and 2,3,4,5,6-pentachlorophenyl (PCP)-O-dG were obtained in this manner.

Further optimization of the synthesis was carried out by the Manderville laboratory (Scheme 1b) and involved replacement of the O^6−Bn protecting group in **1** with the trimethylsilylethyl group. Thus, with **2** as substrate (prepared according to literature procedures[31]) nucleophilic displacement of Br^- by phenolate in xylenes was then followed by TBAF treatment for removal of all protecting groups in a single step. This procedure was used for the preparation of Ph-O-dG, 2-Cl-Ph-O-dG and 2,4-dichlorophenyl (DCP)-O-dG.

Hydrolysis Kinetics and Activation Parameters. A spectrophotometric procedure was used to determine rates of hydrolysis for the *O*-linked 8-dG adducts, as previously carried out for the corresponding *C*-linked analogues.[19] At neutral pH Ph-O-dG has λ_{max} at ∼250 nm with a shoulder peak at ∼284 nm (bold trace, Figure 2a). The deglycosylated nucleobase Ph-O-G shows greater absorbance at ∼280 nm at pH 7 (dashed trace) that shifts to λ_{max} at ∼275 nm at pH 1.0 (dotted trace, Figure 2a). Figure 2b shows changes in absorbance spectra of

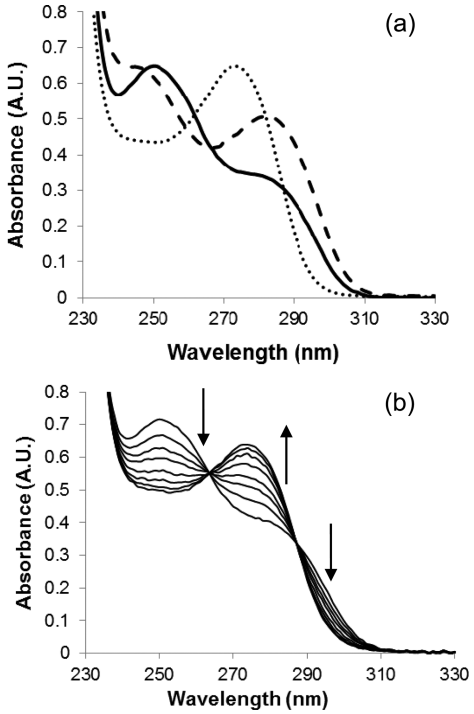

Figure 2. (a) Absorbance spectrum of Ph-O-dG (solid line) and Ph-O-G (dashed line) in pH 7 MOPS buffer (0.05 M, 0.31 M NaCl) and Ph-O-G (dotted line) in pH 1 KCl/HCl (0.2 M). (b) Changes in absorbance spectra of Ph-O-dG in pH 1 buffer (0.2 M KCl/HCl) recorded in 30 s intervals.

Ph-O-dG in pH 1 buffer. The arrows indicate loss of absorbance at 250 nm for Ph-O-dG and gain of absorbance at 275 nm, which correlated with λ_{max} for Ph-O-G in pH 1 buffer (Figure 2a). These spectral changes were consistent with acid-catalyzed hydrolysis of Ph-O-dG into the deglycosylated product Ph-O-G, and this was confirmed by reverse-phase HPLC analysis (Figure S1, Supporting Information).

First order rate constants of hydrolysis (k_{obs}) and half-lives ($t_{1/2}$) were initially determined for all *O*-linked adducts depicted in Scheme 1 by monitoring in pH 1 buffer (0.2 M KCl/HCl) at 37 °C the appearance of a peak corresponding to the deglycosylated base (λ_{max} ∼ 275 nm) as a function of time (Table 1). All *O*-linked 8-dG adducts hydrolyzed at a faster rate than dG. Using Ph-O-dG as the reference point, the derivatives bearing electron-donating groups (4-Me- and 4-MeO-Ph-O-dG) showed little deviation from the rate of Ph-O-dG, while the addition of Cl-substituents retarded the rate of hydrolysis at pH 1. The addition of one chlorine atom to the phenyl moiety increased the half-life by ∼30%; upon increased chlorination the half-lives increased further with PCP-O-dG having a half-life ∼8-fold larger than Ph-O-dG. Of the adducted phenolic moieties, PCP is the most electron-withdrawing and was expected to stabilize the developing negative charge on N^9 (Figure 1), thus increasing the rate of hydrolysis.[13,14,19] Conversely, however, the electronegativity of chlorinated phenolic moieties would decrease the N^7H^+ pK_a values, resulting in a lower concentration of protonated adducts at pH 1.0.[13,14]

Gibbs energy of activation ($\Delta G^{\ddagger}$), enthalpy of activation ($\Delta H^{\ddagger}$) and entropy of activation ($\Delta S^{\ddagger}$) for the depurination of the 8-phenoxide-subsitituted nucleosides (Table 1) were extracted from Eyring plots (Figure S2, Supporting Informa-

dx.doi.org/10.1021/jo401122j | J. Org. Chem. 2013, 78, 7176−7185

Table 1. Summary of First-Order Rate Constants (k_{obs}), Half-lives ($t_{1/2}$), and Activation Parameters for Hydrolysis of *O*-Linked 8-dG Adducts in pH 1 Buffer

adduct	k_{obs} (min^{-1}), $t_{1/2}$ (min)[b]	$k/k_{(dG)}$	$\Delta G^{\ddagger}$ (kcal/mol)[c]	$\Delta H^{\ddagger}$ (kcal/mol)	$\Delta S^{\ddagger}$ (eu)
Ph-O-dG	1.11 ± 0.04, 0.63	28	18.2	19.8 ± 0.5	5.5 ± 1.5
4-Me-Ph-O-dG	1.178 ± 0.003, 0.59	30	18.1	19.7 ± 0.3	5.4 ± 0.7
4-MeO-Ph-O-dG	1.152 ± 0.006, 0.60	29	18.1	19.8 ± 0.1	5.6 ± 0.3
4-Cl-Ph-O-dG	0.81 ± 0.05, 0.85	21	18.3	20.1 ± 0.1	6.1 ± 0.8
2-Cl-Ph-O-dG	0.871 ± 0.008, 0.80	22	18.3	20.0 ± 0.1	5.5 ± 0.6
DCP-O-dG	0.51 ± 0.02, 1.36	13	18.6	19.7 ± 0.1	3.7 ± 0.2
TCP-O-dG	0.260 ± 0.008, 2.66	6.7	19.0	20.0 ± 0.1	3.5 ± 0.2
PCP-O-dG	0.145 ± 0.004, 4.77	3.7	19.5	21.6 ± 0.3	7.1 ± 1.1
dG[a]	0.0391, 17.7	1	21.2	22.5	4.3

[a]Data for dG are taken from ref 6. [b]Determined in pH 1 buffer (0.2 M KCl/HCl) at 37 °C from an average of six kinetic runs. [c]Calculated from $\Delta G^{\ddagger} = \Delta H^{\ddagger} - T\Delta S^{\ddagger}$ at 25 °C.

tion) of rate as a function of temperatures (Table S1, Supporting Information). Activation parameters have been determined previously for hydrolysis of dG in 0.1 M HCl (pH ∼ 1),[6] and are shown in Table 1 for comparison. The $\Delta G^{\ddagger}$ values for *O*-linked 8-dG adducts are all lower than for dG ($\Delta G^{\ddagger}$ = 21.2 kcal/mol), as the most stable adduct PCP-O-dG hydrolyzed 3.7 times faster than dG, indicating a lower activation barrier. The $\Delta S^{\ddagger}$ values do not show any particular trend; however, they are all small positive values, suggesting a late transition state, whereby the glycosidic bond is breaking to create more disorder in the system. Overall, the activation parameters for the *O*-linked 8-dG adducts are consistent with parameters for the hydrolysis of purine deoxynucleosides, and the magnitudes are comparable.[6]

Figure 3 shows a plot of log $k_{obs}/k_{obs(Ph\text{-}O\text{-}dG)}$ versus Hammett substituent constant σ for hydrolysis of the *O*-linked

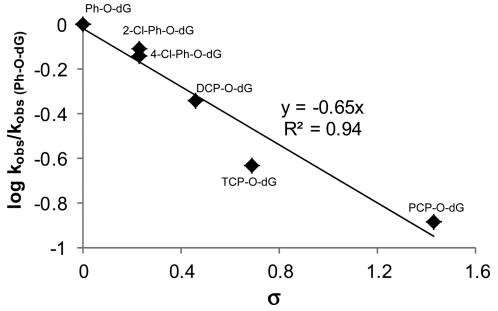

Figure 3. Hammett plot for *O*-linked phenolic 8-dG adducts using σ vs log $k_{obs}/k_{obs(Ph\text{-}O\text{-}dG)}$ in pH 1 buffer (0.2 M KCl/HCl) at 37 °C.

chlorophenolic 8-dG adducts using the rate data presented in Table 1. For adducts containing more than one Cl-substituent, σ is the sum of the individual contributions of each Cl in the adduct:[32] values of σ_m and σ_p of 0.37 and 0.23 are taken from the literature.[33] For ortho Cl groups it was assumed that steric effects are largely absent. Under this scenario, ortho substituents have similar electronic influences as para substuents;[34−37] therefore, σ_p values were also utilized for σ_o. The resulting plot yielded a negative slope (ρ) of −0.65 with a good linear correlation of R^2 = 0.94. The negative reaction constant ρ suggests that the reaction rate is determined by the step that includes a buildup of positive charge, the pre-equilibrium established in the first step of the acid-catalyzed deglycosylation mechanism (Figure 1a). At pH 1 it is unlikely that *O*-linked adducts form dicationic species given that pK_{a2} for dG is ∼ −2.5.[38] Under conditions where involvement of the diprotonated species can be ignored, $k_1 \approx k_{obs}K_{a1}/[H^+]$.[5,6] Thus, log k_{obs} = log k_1 − log K_{a1} + log $[H^+]$ and log $k_{obs} = \sigma\rho \approx \sigma\rho k_1 - \sigma\rho K_{a1}$ + constant (log $[H^+]$). Electron-withdrawing substituents favor bond cleavage (k_1)[14,19] as well as dissociation of the acid (K_{a1})[37] and provide positive ρ values in Hammett plots. The negative slope observed for the Hammett plot (Figure 3) implies that $\sigma\rho K_{a1}$ is larger than $\sigma\rho k_1$ at pH 1. Previously, Hammett analysis for the *C*-linked 8-dG adducts at ∼ pH 1 showed a small positive slope of 0.54.[19] In this case the pH of the solution was well below N^7H^+ pK_a values for the *C*-linked 8-dG adducts. However, at pH 4, where pH > pK_{a1}, the Hammett analysis for the *C*-linked 8-dG adducts provided a negative slope.[39] The Hammett plot shown in Figure 3 implied surprisingly low N^7H^+ pK_a values (<1) for the *O*-linked 8-dG adducts.

Proton Affinity (PA). Efforts to determine ionization constants for *O*-linked 8-dG adducts in a low pH range (0.5−4 in aqueous buffered media) were carried out at 25 °C using the spectrophotometric procedure. Overlay absorption spectra for Ph-O-dG as a function of pH showed an increase in absorbance at 273 nm as the solution acidity increased. By plotting the initial absorbance at 273 nm as a function of pH for Ph-O-dG (Figure S3, Supporting Information), a pK_a value of 1.1 ± 0.2 was obtained for the protonated species. This value is more than 1 pH unit below the pK_a of N^7H^+-dG (2.34).[8] For

Table 2. Ionization Constants for 2-Phenoxypyridines and *O*-Linked 8-dG Adducts Used for Determination of First-Order Rate Constants (k_1) at pH 1

compound	NH^+ pK_a[a]	ΔpK_a	adduct	N^7H^+ pK_a	K_a	k_1 (min^{-1})[e]
Ph-O-pyr	2.24 ± 0.05	−3.01[b]	Ph-O-dG	1.1 ± 0.2[a]	0.079	0.87
4-Cl-Ph-O-pyr	2.05 ± 0.07	−0.18[c]	4-Cl-Ph-O-dG	0.92[d]	0.12	0.97
DCP-O-pyr	1.51 ± 0.06	−0.73[c]	DCP-O-dG	0.37[d]	0.43	2.2

[a]Obtained from spectrophotometric titration at 25 °C from an average for three independent measurements. [b]Compared to literature pK_a value (ref 40) for pyridine. [c]Compared to pK_a value determined for Ph-O-pyr. [d]Estimated value from pK_a = pK_a Ph-O-dG (1.1) + ΔpK_a (−0.18 or −0.73). [e]Recorded at pH 1 where $k_1 \approx k_{obs}K_{a1}/[H^+]$.

dx.doi.org/10.1021/jo401122j | J. Org. Chem. 2013, 78, 7176−7185

the chlorophenolic *O*-linked 8-dG adducts, accurate pK_a values could not be determined because of the weakly basic nature of N^7, coupled with competitive hydrolysis of the adduct in strongly acidic media. To provide surrogate information on the impact of the phenoxy substituent on N^7 basicity, 2-phenoxypyridine analogues (Ph-O-pyr, 4-Cl-Ph-O-pyr and DCP-O-pyr) were prepared as model compounds, and their proton affinity was analyzed using the spectrophotometric procedure. The sp^2-hybridized ring nitrogen of pyridine is much more basic than N^7 of dG, possessing a pK_a of 5.25 for its conjugate acid,[40] and the pyridine derivatives do not undergo hydrolysis under our experimental conditions. Thus, pK_a values for the conjugate acids of Ph-O-pyr, 4-Cl-Ph-O-pyr and DCP-O-pyr were easier to determine with accuracy compared to their corresponding monoprotonated 8-dG adducts. Spectrophotometric titrations of the 2-phenoxypyridine analogues (Figure S4, Supporting Information) provided the pK_a values for the conjugate acids given in Table 2. The pK_a of the conjugate acid of Ph-O-pyr was ∼2.24 for a ΔpK_a value of −3.01 relative to the conjugate acid of pyridine. 4-Cl-Ph-O-pyr and DCP-O-pyr have pK_a values for the conjugate acids of 2.05 and 1.51, respectively. For comparison, the pK_a for the conjugate acid of 2-chloropyridine is ∼0.5.[40]

The ΔpK_a values of −0.18 and −0.73 for 4-Cl-Ph-O-pyr and DCP-O-pyr relative to Ph-O-pyr (Table 2) provided a measure on how these Cl-substituted phenoxy ring systems impact the basicity of the adjacent sp^2-hybridized N atom. Given that Ph-O-dG possesses a pK_a ∼ 1.1 for its conjugate acid, the ΔpK_a values were used to estimate the N^7H^+ pK_a values for 4-Cl-Ph-O-dG and DCP-O-dG (i.e., pK_a = pK_a Ph-O-dG (1.1) + ΔpK_a (−0.18 or −0.73)) and were calculated to be 0.92 and 0.37, respectively. Utilizing the K_a values, k_1 values of 0.87, 0.97, and 2.2 min^{-1} were determined for the three *O*-linked adducts at pH 1 (Table 2). The increase in k_1 upon addition of Cl groups is the expected trend for addition of electron-withdrawing substituents to the 8-position of dG.[13,14,19]

Our experimental findings suggested that increased Cl-substitution of the phenyl ring in *O*-linked 8-dG adducts diminishes the rate of hydrolysis at pH 1 by lowering N^7 basicity. However, protonation at N^3 may compete effectively for protonation at N^7 for some *O*-linked 8-dG adducts, and this would influence the hydrolysis reaction. Given our inability to distinguish N^7 from N^3 protonation using spectrophotometric techniques, DFT calculations were used to determine structures of the protonated species (i.e., Figure 4) and determine gas-phase and solvent-phase (water) proton affinities (PA, kcal·mol^{-1}) for both N^7H^+ and N^3H^+ adducts (Table 3). For dG, the *anti*-conformation is the most stable structure for both the neutral and N^7H^+ species (Table 3). However, the *syn*-conformation is favored for the N^3H^+ species due to H-bonding interaction between 5′-O of the sugar moiety and N^3H. For the *O*-linked 8-dG adducts, the *syn*-conformation is the most stable structure (Figure 4, Table 3), which reduces steric interactions between the phenolic ring and sugar moiety and favors H-bonding interactions between 5′-OH and N^3 (Figure 4). On the basis of terminology for describing biaryl ether conformation,[41] neutral Ph-O-dG (Figure 4), 4-Cl-Ph-O-dG and DCP-O-dG (Table 3) were present in a planar conformation, while neutral TCP-O-dG (Table 3) and PCP-O-dG (Figure 4) adopted a skew conformation that diminishes steric interactions between the dG moiety and the TCP and PCP ring system. All *O*-linked 8-dG adducts adopt a skew conformation when protonated at both N^7 and N^3 (Table 3, Figure 4).

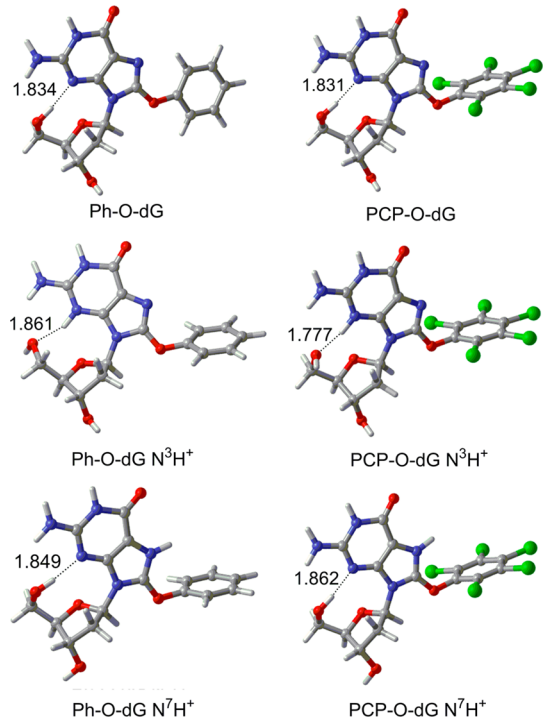

Figure 4. The most stable B3LYP/6-311+G(2df,p)//B3LYP/6-31G(d) conformers for the Ph-O-dG and PCP-O-dG adducts, as well as their N^3-(N^3H^+) and N^7-(N^7H^+) protonated analogues (Select hydrogen bond lengths (Å) are provided).

Table 3. Low-Energy Conformations[a] and Proton Affinities (PA, kcal·mol^{-1}) at the N^3 and N^7 Site of *O*-Linked 8-dG adducts[b]

adduct	neutral	N^7H^+	N^3H^+	N^3 $PA_{(gas)}$	N^3 $PA_{(water)}$	N^7 $PA_{(gas)}$	N^7 $PA_{(water)}$
Ph-O-dG	*syn*-planar	*syn*-skew	*syn*-skew	219.8	257.8	227.8	259.6
4-Cl-Ph-O-dG	*syn*-planar	*syn*-skew	*syn*-skew	217.9	257.4	225.2	258.8
DCP-O-dG	*syn*-planar	*syn*-skew	*syn*-skew	219.1	259.1	223.9	258.0
TCP-O-dG	*syn*-skew	*syn*-skew	*syn*-skew	219.1	257.4	223.2	254.8
PCP-O-dG	*syn*-skew	*syn*-skew	*syn*-skew	218.0	257.4	221.3	253.8
dG	*anti*	*anti*	*syn*	216.6	255.7	232.1	260.8

[a]The most stable B3LYP/6-311+G(2df,p)//B3LYP/6-31G(d) conformers for the neutral, N^7-(N^7H^+) and N^3-(N^3H^+) protonated analogues. [b]N^3 and N^7 proton affinity (PA) was calculated as the negative of the enthalpy change for protonation (kcal·mol^{-1}).

In the gas-phase the calculated N^7 PA for dG is 232.1 kcal·mol^{-1} (Table 3), which is similar to the experimental PA (234.4 kcal·mol^{-1}),[42] and is ∼15.5 kcal·mol^{-1} above the gas-phase N^3 PA; a calculated value of ∼20 kcal·mol^{-1} has been previously reported.[43] In water the DFT calculations still predict a preference for N^7-protonation of dG, but the energy difference between the PA of N^7 and N^3 is only ∼5 kcal·mol^{-1} (Table 3). Attachment of the phenoxy substituent to C^8 of dG to afford Ph-O-dG decreases the gas-phase N^7 PA by 4.3 kcal·mol^{-1}, and raises N^3 PA by 3.2 kcal·mol^{-1}. The gas-phase

dx.doi.org/10.1021/jo401122j | J. Org. Chem. 2013, 78, 7176−7185

calculations indicate a strong preference for N^7-protonation (favored by 8 kcal·mol^{-1}) of Ph-O-dG, while in water the preference for N^7-protonation is only favored by 1.8 kcal·mol^{-1}. Attachment of Cl-substituents to the phenyl ring further diminishes N^7 PA, with PCP-O-dG having a gas-phase N^7 PA of 221.3 kcal·mol^{-1}, which is 6.5 kcal·mol^{-1} below N^7 PA for Ph-O-dG. In contrast, N^3 PA is not strongly influenced by Cl-substitution, and the gas-phase N^3 PA is ∼218−220 kcal·mol^{-1} for all *O*-linked adducts, which is 1.4−3.2 kcal·mol^{-1} above N^3 PA calculated for dG. This difference may stem from the fact that dG is the only base that undergoes a conformational change (*anti* → *syn*) upon N^3-protonation. In water the calculations predict N^3 to have a greater PA than N^7 for DCP-O-dG, TCP-O-dG and PCP-O-dG. Thus, for these *O*-linked adducts, protonation at N^3 may compete effectively for protonation at N^7, and this would influence the hydrolysis reaction.

Influence of Protonation Site on Deglycosylation. Given that DFT calculations predict a greater N^3 PA than N^7 PA for DCP-O-dG, TCP-O-dG and PCP-O-dG (Table 3), it was desirable to determine the influence of protonation site on the deglycosylation barrier. Figure 5 shows the calculated deglycosylation profile for Ph-O-dG (purple trace), 4-Cl-Ph-O-dG (blue trace), DCP-O-dG (green trace), TCP-O-dG (orange trace) and PCP-O-dG (red trace), as well as the corresponding N^3- and N^7-protonated species (kJ·mol^{-1}). The calculations predict that N^7-protonation has a much larger effect on the barrier for deglycosylation than does N^3-protonation. In water (Figure 5a), the barrier for the N^7-protonated *O*-linked adducts is from ∼60−80 kJ·mol^{-1}, while the barrier for the N^3-protonated adducts is ∼100−120 kJ·mol^{-1} that is further increased to ∼140 kJ·mol^{-1} for the neutral adducts. For each species (neutral, N^3H^+ and N^7H^+), the calculations predict PCP-O-dG to possess the lowest barrier, followed by TCP-O-dG, DCP-O-dG, 4-Cl-Ph-O-dG and finally Ph-O-dG. In the gas-phase (Figure 5b), the deglycosylation barrier is slightly diminished for the N^7-protonated adducts versus the corresponding barrier in water, while the barrier for the N^3-protonated adducts is increased and is comparable to the neutral adducts. These calculations imply that the chlorophenoxyl substituents could influence the site of protonation to generate N^3H^+ adducts that are relatively stable to hydrolysis compared to their N^7H^+ counterparts. This possibility cannot be ruled out and may provide a rationale for the relative stability of PCP-O-dG in aqueous media at pH 1.

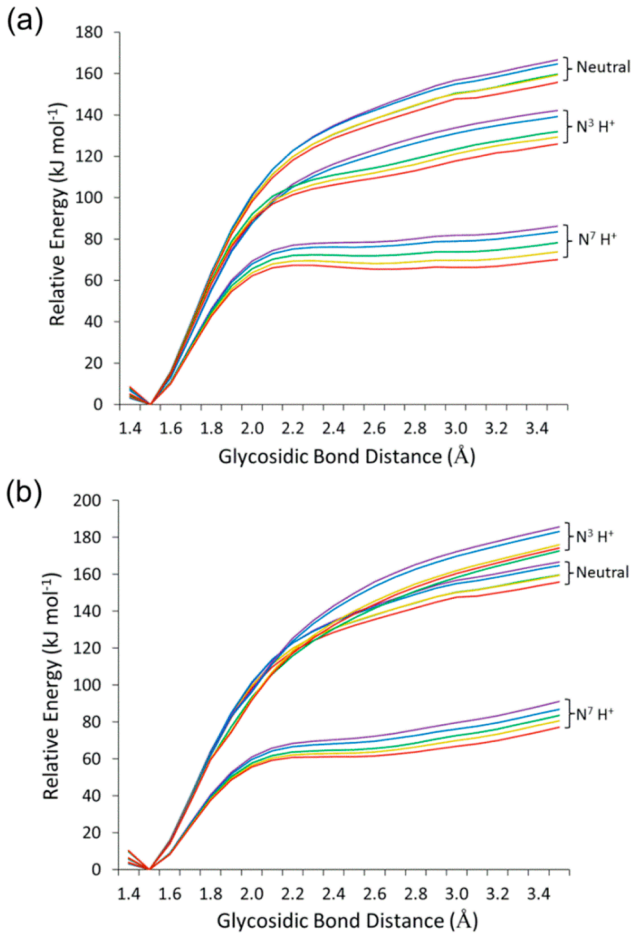

Figure 5. Constrained IEF-PCM-B3LYP/6-31G(d) deglycosylation barriers calculated in (a) water and (b) the gas phase for Ph-O-dG (purple), 4-Cl-Ph-O-dG (blue), DCP-O-dG (green), TCP-O-dG (orange) and PCP-O-dG (red), as well as the corresponding N^3-(N^3 H^+) and N^7-(N^7 H^+) protonated species (kJ·mol^{-1}).

Gas-Phase Deglycosylation. Further insight into the influence of Cl-substitution on the hydrolysis of the *O*-linked 8-dG adducts was accomplished using electrospray positive ionization (ESI^+) mass spectrometry. The deglycosylation barriers predicted by DFT calculations suggested PCP-O-dG to be the most reactive, while hydrolysis kinetics in aqueous media at pH 1 showed PCP-O-dG to be the least sensitive to acid-catalyzed hydrolysis of the *O*-linked adducts. In the DFT calculations, barriers were determined for the monoprotonated species, while the hydrolysis kinetics is influenced by the pre-equilibrium established in the first step of the acid-catalyzed deglycosylation mechanism. Thus, it was desirable to use an experimental technique such as ESI-MS that can isolate monoprotonated adducts and determine their relative stability to deglycosylation. These relative gas-phase stabilities can be expressed as the percentage of deglycosylated product as determined by the relative peak intensities between the parent ion $[M + H]^+$ and deglycosylated product ion $[M - 116 + H]^+$ by ESI^+-MS/MS. It is important to note that in this experiment, we assumed that the ionization potential of the parent ion and deglycosylation product ion were the same across each adduct tested.

Figure 6a shows the ESI^+-MS/MS spectrum of 4-Cl-Ph-O-dG. The adduct shows an $[M + H]^+$ ion at 394 with loss of 116 mass units corresponding to the deoxyribose sugar moiety to generate a positively charged nucleobase at *m*/*z* 278. This observation was consistent with deglycosylation of the monoprotonated adduct through cleavage of the N-glycosidic bond.[44−46] The percentage of deglycosylated product for 4-Cl-Ph-O-dG was determined to be 28%. Under identical ESI^+-MS/MS conditions the percentage of deglycosylated product for Ph-O-dG and the other chlorinated *O*-linked adducts was determined (Figure 6b). Consistent with the DFT calculations (Figure 5), the monoprotonated Ph-O-dG adduct was the least reactive with only 1.2% deglycosylated product. All chlorinated *O*-linked adducts had monoprotonated species more sensitive to deglycosylation than monoprotonated Ph-O-dG (Figure 6b). However, upon further chlorination of the phenyl ring system the degree of deglycosylation decreased relative to that of 4-Cl-Ph-O-dG with the monoprotonated species of PCP-O-dG showing the lowest percentage of deglycosylated product (9.9%) among the chlorinated analogues.

dx.doi.org/10.1021/jo401122j | J. Org. Chem. 2013, 78, 7176−7185

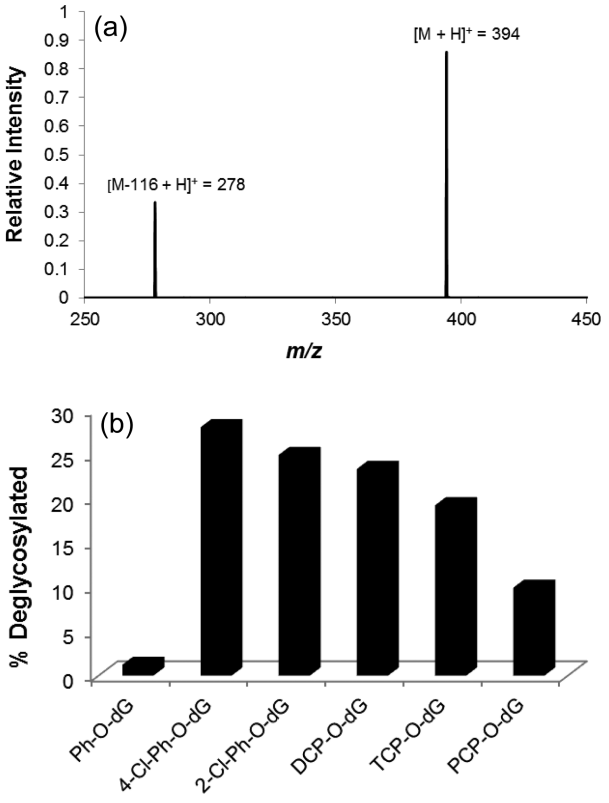

Figure 6. (a) ESI$^+$-MS/MS spectrum of 4-Cl-Ph-O-dG. (b) Relative gas-phase stabilities of *O*-linked 8-dG adducts are expressed as % deglycosylated product by determining the relative peak intensities of the parent ion $[M + H]^+$ and deglycosylated product ion $[M\text{-}116 + H]^+$ by ESI$^+$-MS/MS.

The mechanism of deglycosylation for protonated dG by collision-induced dissociation (CID) in MS has recently been explored using deuterium-enriched samples.[44,45] These experiments suggest that fragmentation proceeds from the *syn*-conformation of the N^7H^+-dG species with initial proton transfer from 5′-OH of the sugar moiety to N^3 on the nucleobase.[44,45] This proton transfer generates a dicationic nucleobase and an anionic sugar possessing a negatively charged 5′-alkoxy group. Liu and co-workers suggest that the 5′-alkoxy group performs a nucleophilic attack at the 1′-site to release the protonated nucleobase and form a neutral sugar containing a new 5-membered ring.[44] In contrast, Greisch and co-workers favor a mechanism in which a 5′-alkoxy group deprotonates a 2′-H, resulting in beta-elimination of the nucleobase to produce a sugar byproduct as a neutral species.[45] Regardless of the exact mechanism, the 8-phenoxy substituents in the *O*-linked adducts appear well removed from the 1′-N^9 reaction site (i.e., Figure 4). Thus, steric interference of deglycosylation by increased Cl substitution is unlikely to play a major role in the relative percent deglycosylated product observed by ESI$^+$-MS. Instead, electronic factors are proposed to play a main role. For TCP-O-dG and especially PCP-O-dG, parent ions may contain both N^3H^+ and N^7H^+ ions and increased involvement of N^3H^+ ions will increase the deglycosylation barrier (Figure 5) and hence decrease the percent deglycosylated product (Figure 6).

Hydrolysis at Neutral pH. To gain insight into hydrolysis rates at neutral pH, hydrolysis kinetics between pH 0.8−2.5 for Ph-O-dG and DCP-O-dG at 55 °C (Figure S5, Supporting Information) were constructed and afforded straight lines, indicating continuous first-order dependence on H^+ activity.[13,19] Experimental limitations for obtaining rates over a broader range of pH values included the limited solubility of *O*-linked adducts, especially chlorinated analogues, at pH values ≥2.5, and the inhibition of hydrolysis when using CH_3CN as cosolvent to enhance solubility. To provide an estimate of rates at neutral pH for *O*-linked adducts, the pH-rate profiles were extrapolated to pH 7 to render rates of 6×10^{-9} min^{-1} ($t_{1/2} \approx$ 220 years) and 3×10^{-10} min^{-1} ($t_{1/2} \approx$ 4395 years) for Ph-O-dG and DCP-O-dG, respectively, at 55 °C. For comparison, a similar estimate for the rate of hydrolysis of the *C*-linked 8-Ph-dG nucleoside adduct at neutral pH is $\sim 1.90 \times 10^{-5}$ min^{-1} ($t_{1/2} \approx$ 25 days) at 37 °C.[19] For *N*-linked 8-dG adducts, rates of hydrolysis at neutral pH are as high as 5.2×10^{-7} s^{-1} ($t_{1/2} \approx$ 15 days) at 20 °C.[18] A corresponding rate for dG at 20 °C is estimated at $\sim 1.2 \times 10^{-9}$ s^{-1} ($t_{1/2} \approx$ 6,684 days).[18] The inclusion of our data on the stability of *O*-linked adducts now establishes that the order of hydrolytic reactivity at neutral pH for bulky 8-dG adducts is *N*-linked > *C*-linked > *O*-linked, which correlates with their relative ease of N^7-protonation.

CONCLUSIONS

The current study has allowed us to conclude the following: (1) *O*-linked 8-dG adducts produced by phenols are resistant to hydrolysis under physiological conditions and are unlikely intermediates leading to abasic site formation. (2) Their resistance to hydrolysis stems from the ability of the phenoxy substituent to diminish N^7 proton affinity, which is supported by both experimental pK_a values and calculated proton affinities (PAs) in gas- and solvent- (water)-phase. (3) In water at pH 1, increased Cl-substitution diminishes the rate of hydrolysis by disfavoring N^7-protonation in the pre-equilibrium established in the first step of the acid-catalyzed deglycosylation mechanism. This trend is supported by the Hammett plot, which shows a linear negative slope with $\rho_X = -0.65$. However, DFT calculations show that the barrier to deglycosylation becomes progressively smaller for N^7H^+ adducts bearing increased numbers of Cl-substituents. This observation follows the general trend for hydrolysis of 8-dG adducts; electron-withdrawing 8-substituents increase the rate of depurination through stabilization of the developing negative charge at N^9 during rate-limiting cleavage of the glycosyl bond. (4) The degree of deglycosylation induced by CID in ESI$^+$-MS demonstrate that all *O*-linked 8-dG adducts containing Cl-substituents are more prone to deglycosylation than the unsubstituted analogue Ph-O-dG in the gas-phase. However, within the chlorinated analogues, 4-Cl-Ph-O-dG showed the greatest percent deglycosylation, and progressive addition of Cl-substituents to generate PCP-O-dG diminished the extent of deglycosylation. DFT calculations suggest that N^3-protonation may compete effectively with N^7-protonation for both TCP-O-dG and PCP-O-dG, and monoprotonated N^3H^+ species possess much greater barriers to deglycosylation than their N^7-protonated counterparts.

EXPERIMENTAL SECTION

Materials and Methods. Anhydrous 1,4-dioxane was distilled over Na. Xylenes and pyridine were distilled over CaH_2 and stored under nitrogen. Other commercial compounds were used as received. *O*-Linked 8-dG adducts 4-Me-Ph-O-dG, 4-OMe-Ph-O-dG, TCP-O-dG and PCP-O-dG were synthesized as previously reported and were >95% pure by ^{1}H NMR.[30] The synthesis of 8-bromo-2′-deoxyguano-

dx.doi.org/10.1021/jo401122j | J. Org. Chem. 2013, 78, 7176−7185

sine (8-Br-dG) was performed, as outlined previously,[47] by treating dG with *N*-bromosuccinimide in a water−acetonitrile mixture. 8-Bromo-3′,5′-*O*-bis(*tert*-butyldimethylsilyl)-2′-deoxyguanosine was prepared according to literature procedures by treating 8-Br-dG with excess *tert*-butyl(chloro)dimethylsilane and imidazole in DMF.[31] NMR spectra were recorded on 300 and 600 MHz spectrometers in either DMSO-d_6, $CDCl_3$ or CD_2Cl_2 referenced to the respective solvent. High-resolution mass spectra (HRMS) were recorded on a Q-TOF instrument, operating in nanospray ionization at 0.5 μL/min detecting positive ions.

8-Bromo-3′,5′-*O*-bis(*tert*-butyldimethylsilyl)-O^6-(trimethylsilylethyl)-2′-deoxyguanosine (2). Compound **2** was prepared by treating 8-bromo-3′,5′-*O*-bis(*tert*-butyldimethylsilyl)-2′-deoxyguanosine (2 g, 3.48 mmol) with triphenylphosphine (4.6 g, 17.4 mmol), 2-(trimethylsilyl)-ethanol (2.5 mL, 17.4 mmol) and diisopropyl azodicarboxylate (DIAD) (3.4 mL, 17.4 mmol) in anhydrous dioxane, as outlined previously.[31] The crude product was purified by silica gel column chromatography (Hex:EtOAc 20:1 to 10:1) to yield 1.5 g (64%) of a colorless oil: ^{1}H NMR (300 MHz, $CDCl_3$) δ 6.24 (t, J = 6.9 Hz, 1H), 4.75 (m, 1H), 4.70 (bs, 2H), 4.50 (m, 2H), 3.90 (m, 1H), 3.85 (m, 1H), 3.67 (dd, J = 10.2, 4.3 Hz, 1H), 3.52 (m, 1H), 2.14 (m, 1H) 1.18 (m, 2H), 0.91 (s, 9H), 0.83 (s, 9H), 0.12 (s, 6H), 0.06 (s, 9H), 0.01 (s, 3H), −0.03 (s, 3H); ^{13}C NMR (151 MHz, $CDCl_3$) δ 160.2, 158.5, 154.1, 125.6, 116.5, 87.3, 85.6, 72.3, 65.0, 62.7, 36.3, 25.8, 18.3, 18.0, 17.5, −1.5, −4.6, −4.7, −5.43, −5.5; MS (ESI) calcd for $C_{27}H_{53}BrN_5O_4Si_3$ 674.3, found m/z 674.3 (MH^+).

General Method for *O*-Linked 8-dG Adduct Synthesis. Compound **2** was added to a round bottomed flask with 4 equiv of the desired phenol and 2 equiv of finely ground K_3PO_4. The reaction vessel was sealed and purged with argon, prior to adding 8 mL of distilled xylenes. The reaction was then stirred and heated at 130 °C for ∼17 h. After completion, 25 mL of EtOAc was added, and the mixture was washed with 2 × 50 mL saturated bicarbonate solution, followed by 50 mL of water. The organic layer was dried over Na_2SO_4 and concentrated in vacuo. To the crude product was added 3 equiv of TBAF·3H_2O and 5 mL of reagent grade THF. THF was removed in vacuo, and the crude product was purified by silica gel chromatography (10% methanol in methylene chloride) to yield the *O*-linked nucleoside adduct in ≥95% purity, as evidenced by ^{1}H NMR.

8-Phenoxy-2′-deoxyguanosine (Ph-O-dG). 8-Phenoxy-2′-deoxyguanosine (Ph-O-dG)[30] was synthesized from compound **2** (1 g, 1.48 mmol), phenol (0.56 g, 5.92 mmol), and K_3PO_4 (0.63g, 2.96 mmol) followed by deprotection with TBAF·3H_2O (1.4 g, 4.44 mmol) to yield 0.38 g of a white solid (73% over two steps): mp 148 °C decomp.; ^{1}H NMR (600 MHz, DMSO-d_6) δ 10.68 (bs, 1H), 7.44 (t, J = 8.5 Hz, 2H), 7.31 (d, J = 7.8 Hz, 2H), 7.25 (t, J = 7.4 Hz, 1H), 6.45, (s, 2H), 6.21 (t, J = 7.3 Hz, 1H), 5.27 (d, J = 4.0 Hz, 1H), 4.85 (t, J = 5.9 Hz, 1H), 4.34 (m, 1H), 3.77 (m, 1H), 3.50 (m, 1H), 3.44 (m, 1H), 2.91 (m, 1H), 2.15 (m, 1H); ^{13}C NMR (151 MHz, DMSO-d_6) δ 155.8, 153.5, 153.3, 149.8, 149.0, 129.7, 125.2, 119.8, 110.7, 87.4, 81.8, 70.9, 62.0, 36.6; HRMS (ESI) calcd for $C_{16}H_{18}N_5O_5$ 360.1308, found 360.1304 (MH^+).

8-(2-Chlorophenoxy)-2′-deoxyguanosine (2Cl-Ph-O-dG). 8-(2-Chlorophenoxy)-2′-deoxyguanosine (2Cl-Ph-O-dG) was synthesized from compound **2** (0.2 g, 0.30 mmol), 2-chlorophenol (0.15 g, 1.18 mmol), and K_3PO_4 (0.13 g, 0.59 mmol) followed by deprotection with TBAF·3H_2O (0.28 g, 0.88 mmol) to yield 0.08 g of a white solid (68% over two steps): mp 135 °C decomp.; ^{1}H NMR (300 MHz, DMSO-d_6) δ 10.62 (bs, 1H), 7.62 (d, J = 6.6 Hz, 1H), 7.44 (m, 2H), 7.33 (m, 1H) 6.42, (bs, 2H), 6.22 (t, J = 7.1 Hz, 1H), 5.25 (d, J = 4.1 Hz, 1H), 4.79 (t, J = 5.9 Hz, 1H), 4.32 (m, 1H), 3.77 (m, 1H), 3.46 (m, 2H), 2.94 (m, 1H), 2.17 (m, 1H); ^{13}C NMR (151 MHz, DMSO-d_6) δ 155.7, 153.4, 150.0, 148.8, 148.7, 130.4, 128.6, 127.3, 125.0, 123.2, 110.6, 87.5, 81.9, 70.9, 62.0, 36.6; HRMS (ESI) calcd for $C_{16}H_{17}ClN_5O_5$ 394.0918, found 394.0913 (MH^+).

8-(2,4-Dichlorophenoxy)-2′-deoxyguanosine (DCP-O-dG). 8-(2,4-Dichlorophenoxy)-2′-deoxyguanosine DCP-O-dG was synthesized from compound **2** (0.22 g, 0.388 mmol), 2,4-dichlorophenol (0.22 g, 1.34 mmol), and K_3PO_4 (0.14 g, 0.66 mmol) followed by deprotection with TBAF·3H_2O (0.42g, 1.3 mmol) to yield 0.13 g of a white solid (80% over two steps): mp 155 °C decomp.; ^{1}H NMR (300 MHz, DMSO-d_6) δ 10.64 (s, 1H), 7.81 (s 1H), 7.53, (m, 2H), 6.44, (bs, 2H), 6.21 (t, J = 7.3 Hz, 1H), 5.25 (d, J = 4.1 Hz, 1H), 4.79 (t, J = 5.9 Hz, 1H), 4.32 (m, 1H), 3.76 (m, 1H), 3.47 (m, 1H), 3.43 (m, 1H), 2.92 (m, 1H), 2.15 (m, 1H); ^{13}C NMR (151 MHz, DMSO-d_6) δ 155.7, 153.5, 150.1, 148.5, 147.8, 130.6, 129.9, 128.7, 126.2, 124.5, 110.6, 87.5, 81.9, 70.9, 62.0, 36.6; HRMS (ESI) calcd for $C_{16}H_{16}Cl_2N_5O_5$ 428.0528, found 428.0522 (MH^+).

8-Phenoxy-guanine (Ph-O-G). 8-Phenoxy-2′-deoxyguanosine (Ph-O-dG, 0.02 g, 0.05 mmol) was added to a round-bottom flask along with 5 mL of 10% formic acid. The mixture was stirred and heated to 75 °C for 1 h. After cooling, 10 mL of water was added, and the pH was adjusted to 6 using 1 M NaOH. The isolated solid (14 mg, 96%) was the formate salt of Ph-O-dG: mp 237 °C decomp.; ^{1}H NMR (300 MHz, DMSO-d_6) δ 10.93 (bs, 1H), 8.45 (s, 1H), 8.29 (s, 1H, (HCOOH)), 7.39 (m, 2H), 7.25 (m, 2H), 7.23 (m, 1H), 6.40 (s, 2H); ^{13}C NMR (151 MHz, DMSO-d_6, partial assignment) δ 165.8 (HCOOH), 154.1, 153.1, 129.5, 124.4, 119.2; HRMS (ESI) calcd for $C_{11}H_{10}N_5O_2$ 244.0834, found 244.0835 (MH^+).

General Method for Synthesis of 2-Phenoxypyridines. 2-Phenoxypyridines were prepared using a microwave-assisted Ullmann ether synthesis reported by D'Angelo and co-workers.[48] 2-Bromopyridine and the desired phenol (1.5 equiv) were suspended in dry DMF (∼4 mL) in a microwave vial. Copper powder (10%) and Cs_2CO_3 (3 equiv) were added, and the system was purged with argon and then placed in the microwave reactor and allowed to react for 10 min at 100 °C and 60 W. The reaction was then cooled to room temperature and diluted with CH_2Cl_2 (25 mL). The organic phase was washed with 1 M NaOH (60 mL) and then 100 mL water, dried over Na_2SO_4, decanted, and concentrated in vacuo. The crude product was purified by silica gel chromatography using (10:2 Hex:EtOAc) to yield the desired 2-phenoxypyridines, which were characterized by NMR spectroscopy.

2-Phenoxypyridine (Ph-O-pyr). Following the general procedure, phenol (1.5 g, 4.6 mmol) and 2-bromopyridine (0.16 mL, 1.6 mmol) provided 0.273 g of Ph-O-pyr[49] as a clear oil (100%): ^{1}H NMR (300 MHz, $CDCl_3$) δ 8.11 (dd, J = 5.0, 1.1 Hz, 1H), 7.57 (td, J = 7.2, 2.0 Hz, 1H), 7.31 (t, J = 6.2 Hz, 2H), 7.28−7.03 (m, 3H), 6.88 (t, J = 5.9 Hz, 1H), 6.79 (d, J = 8.3 Hz, 1H); ^{13}C NMR (151 MHz, $CDCl_3$) δ 163.7, 154.1, 147.8, 139.4, 129.7, 124.6, 121.1, 118.4, 111.5.

2-(4-Chlorophenoxy)pyridine (4Cl-Ph-O-pyr). Following the general procedure 2-bromopyridine (0.155 mL, 1.6 mmol) and 4-chlorophenol (0.31 g, 2.4 mmol) afforded 0.204 g of 4Cl-Ph-O-pyr[50] as a yellow oil (62%): ^{1}H NMR (300 MHz, $CDCl_3$) δ 8.07 (dd, J = 4.4, 1.3 Hz, 1H), 7.56 (td, J = 7.2, 2.0 Hz, 1H), 7.23 (d, J = 6.7 Hz, 2H), 6.98 (d, J = 5.9 Hz, 2H), 6.86 (t, J = 7.2 Hz, 1H), 6.79 (d, J = 8.3 Hz, 1H); ^{13}C NMR (151 MHz, $CDCl_3$) δ 163.3, 152.6, 147.6, 139.5, 129.7, 129.6, 122.6, 118.7, 111.6.

2-(2,4-Dichlorophenoxy)pyridine (DCP-O-pyr). Following the general procedure 2-bromopyridine (0.155 mL, 1.6 mmol) and 2,4-dichlorophenol (0.39 g, 2.4 mmol) yielded 0.157 g of DCP-O-pyr[51] as a clear oil (41%): ^{1}H NMR (300 MHz, CD_2Cl_2) δ 8.15 (dd, J = 4.9, 1.2 Hz, 1H), 7.74 (td, J = 7.2, 2.0 Hz, 1H), 7.49 (d, J = 2.5 Hz, 1H), 7.30 (dd, J = 8.6, 2.5 Hz 1H), 7.17 (d, J = 8.7 Hz, 1H), 7.05−7.00 (m, 2H); ^{13}C NMR (151 MHz, $CDCl_3$) δ 162.6, 148.5, 147.4, 139.6, 130.7, 130.3, 128.2, 128.0, 124.7, 118.8, 111.1.

Kinetics and pK_a Determinations. The kinetic study was carried out using a UV−vis spectrophotometer equipped with a constant temperature water bath. Hydrolysis reactions were followed by monitoring formation of the deglycosylated nucleobase at its absorption maximum (λ_{max}, e.g., 275 nm for Ph-O-G). The reaction was initiated by injection of 20 μL of a 4 mM stock solution (DMSO) of *O*-linked 8-dG adduct into a Teflon-capped 10 mm UV cell containing 1980 μL of aqueous 0.2 M buffer (pH 0.8−2.5) that had been incubated at the appropriate temperature (25, 37, 45, 55, or 65 °C) for 15 min. Measurements were conducted in parallel using the multicell changer, with six first-order rate constant values for hydrolysis obtained for each adduct in each set of conditions to allow for determination of mean ± standard deviation.

dx.doi.org/10.1021/jo401122j | J. Org. Chem. 2013, 78, 7176−7185

UV−vis titrations for pK_a determinations of Ph-O-dG, Ph-O-pyr, 4-Cl-Ph-O-pyr and DCP-O-pyr were carried out at 25 °C. Solutions were prepared using 20 μL of a 4 mM substrate stock solution (DMSO) and 1980 μL of buffer consisting of pH 0.8−1.8 (0.2 M KCl/HCl) or pH 2−5 (0.05 M citric acid, 0.31 M NaCl). pK_a values were obtained as outlined in detail previously,[19] and error was calculated from three independent measurements for determination of mean ± standard deviation.

HPLC Analysis. Confirmation of deglycosylation of Ph-O-dG was accomplished using reverse-phase HPLC. Samples of Ph-O-dG and Ph-O-G standards were prepared from 1 μL of the 40 mM DMSO adduct stock solution and 99 μL of purified water (18.2 MΩ). Samples of Ph-O-dG that were subjected to acid before injection were prepared using 20 μL of the DMSO adduct stock and 1980 μL of 0.1 M HCl. The acidic solution was heated to 40 °C and allowed to react for 5 and 10 min; 100 μL was taken out at the desired time of analysis and directly injected into the HPLC. The compounds were separated on a C18 column (50 × 4.60 mm) with a flow rate of 0.75 mL/min using a gradient running from 95% 50 mM aqueous triethylamine acetate (TEAA, pH 7.2):5% acetonitrile to 30% 50 mM TEAA:70% acetonitrile over 30 min. Adduct detection was accomplished by monitoring the UV absorbance at 258 nm.

ESI-MS. Experiments were carried out using a quadrupole ion trap mass spectrometer in the positive ionization mode with an electrospray ionization source. The MS^n spectra were obtained by collision-induced dissociation (CID) with helium gas after isolation of the appropriate precursor ions. Ionization was carried out using the following settings on the ESI: nebulizer gas flow 40 psi, dry gas 10 L/min, dry temperature 220 °C, spray voltage 4500 V. The scan range was 100−1000 m/z and scan resolution was 8100 m/z/s. Collision energies were 0.36 V for ESI^+-MS/MS experiments. Adduct stock solutions (6 mM in DMSO) were diluted to 0.03 mM with water and introduced, through electrospray, to the quadrupole ion trap using a syringe pump at flow rates of 3−5 μL/min. The collection time for each experiment was 1.0 min (300 scans/min).

Computational Details. An internal coordinate Monte Carlo[52] conformational search was initially performed using HyperChem[53] with the AMBER molecular mechanics force field to determine the preferred conformations of the neutral *O*-linked phenoxyl adduct and the various Cl-substituted analogues, as well as the corresponding N^3- and N^7-protonated equivalents. Partial atomic charges for the AMBER calculations were obtained from the PM3 method. In each case, more than 200 conformers were obtained. From these conformers, the 50 lowest energy conformers were fully optimized with B3LYP/6-31G(d). Subsequently, frequency calculations were performed on the 10 lowest energy B3LYP conformers. The global minimum from this set was identified using B3LYP/6-311+G(2df,p) single-point energies that included B3LYP/6-31G(d) zero-point vibrational energy (ZPVE) corrections. The resulting gas-phase global minima were used to obtain the corresponding solvent (water) phase structures from IEF-PCM B3LYP/6-31G(d) optimizations. The lowest energy gas and solvent phase structures were then used to determine the proton affinity (PA) and the deglycosylation barrier of *O*-linked structures. The B3LYP/6-311+G(2df,p) PA (including B3LYP/6-31G(d) ZPVE corrections) at the N^3 and N^7 sites of the *O*-linked 8-dG adducts were determined in the gas and solvent (water) phases as the negative of the enthalpy change for protonation.[42] To scrutinize the effects of the phenoxyl moiety, Cl-substitution and protonation on sugar loss, the deglycosylation reaction was investigated by altering and fixing the glycosidic bond length (1′−N^9) in 0.1 Å increments from 1.4 to 3.5 Å in both the gas phase and water. All B3LYP calculations were performed using Gaussian 09 revisions A.02[54] and C.01.[55]

■ ASSOCIATED CONTENT

Supporting Information

Figures S1−S5 and Table S1 described in the text, NMR spectra of synthetic samples, and Tables S2−S37 (Cartesian coordinates of global minimum structures for neutral, N^7H^+ and N^3H^+ adducts). This material is available free of charge via the Internet at http://pubs.acs.org.

■ AUTHOR INFORMATION

Corresponding Author

*E-mail: sturla@ethz.ch (S.J.S.); stacey.wetmore@uleth.ca (S.D.W.); rmanderv@uoguelph.ca (R.A.M.).

Notes

The authors declare no competing financial interest.

■ ACKNOWLEDGMENTS

Financial support for this research was provided by the Natural Sciences and Engineering Research Council (NSERC) of Canada, the Canada Research Chair program, the Canada Foundation for Innovation, the Ontario Innovation Trust Fund, and the European Research Council (260341). This research has been facilitated by use of computing resources provided by WestGrid and Compute/Calcul Canada.

■ REFERENCES

(1) Lindahl, T. *Nature* **1993**, *362*, 709−715.
(2) Evans, A. R.; Limp-Foster, M.; Kelley, M. R. *Mutat. Res.* **2000**, *461*, 83−108.
(3) Loeb, L. A.; Preston, B. D. *Annu. Rev. Genet.* **1986**, *20*, 201−230.
(4) Roger, M.; Hotchkiss, R. *Proc. Natl. Acad. Sci. U. S. A.* **1961**, *47*, 654−669.
(5) Zoltewicz, D.; Clark, D. F.; Sharpless, T. W.; Grahe, G. *J. Am. Chem. Soc.* **1970**, *92*, 1741−1750.
(6) Hevesi, L.; Wolfson-Davidson, E.; Nagy, J. B.; Nagy, O. B.; Bruylants, A. *J. Am. Chem. Soc.* **1972**, *94*, 4715−4720.
(7) Zoltewicz, J. A.; Clark, D. F. *J. Org. Chem.* **1972**, *37*, 1193−1197.
(8) Da Costa, C. P.; Sigel, H. *Inorg. Chem.* **2003**, *42*, 3475−3482.
(9) Dutta, S.; Chowdhury, G.; Gates, K. S. *J. Am. Chem. Soc.* **2007**, *129*, 1852−1853.
(10) Gates, K. S.; Nooner, T.; Dutta, S. *Chem. Res. Toxicol.* **2004**, *17*, 839−856.
(11) Hsieh, Y. S.; Chen, B. C.; Shiow, S. J.; Wang, H. C.; Hsu, J. D.; Wang, C. J. *Chem.−Biol. Interact.* **2002**, *140*, 67−80.
(12) Suzuki, N.; Yasui, M.; Geacintov, N. E.; Shafirovich, V.; Shibutani, S. *Biochemistry* **2005**, *44*, 9238−9245.
(13) Hovinen, J.; Glemarec, C.; Sandström, A.; Sund, C.; Chattopadhyaya, J. *Tetrahedron* **1991**, *47*, 4693−4708.
(14) Laayoun, A.; Décout, J.-L.; Lhomme, J. *Tetrahedron Lett.* **1994**, *35*, 4989−4990.
(15) Humphreys, W. G.; Kadlubar, K. K.; Guengerich, F. P. *Proc. Natl. Acad. Sci. U. S. A.* **1992**, *89*, 8278−8282.
(16) Dipple, A. *Carcinogenesis* **1995**, *16*, 437−441.
(17) Patel, D. J.; Mao, B.; Gu, Z.; Hingerty, B. E.; Gorin, A.; Basu, A. K.; Broyde, S. *Chem. Res. Toxicol.* **1998**, *11*, 391−407.
(18) Novak, M.; Ruenz, M.; Kazerani, S.; Toth, K.; Nguyen, T.-M.; Heinrich, B. *J. Org. Chem.* **2002**, *67*, 2303−2308.
(19) Schlitt, K. M.; Sun, K. M.; Paugh, R. J.; Millen, A. L.; Navarro-Whyte, L.; Wetmore, S. D.; Manderville, R. A. *J. Org. Chem.* **2009**, *74*, 5793−5802.
(20) Kikugawa, K.; Kato, T.; Kojima, K. *Mutat. Res.* **1992**, *268*, 65−75.
(21) Dai, J.; Wright, M. W.; Manderville, R. A. *J. Am. Chem. Soc.* **2003**, *125*, 3716−3717.
(22) Kornyushyna, O.; Stemmler, A. J; Graybosch, D. M.; Bergenthal, I.; Burrows, C, J. *Bioconjugate Chem.* **2005**, *16*, 178−183.
(23) Rogan, E. G.; Cavalieri, E. L.; Tibbels, S. R.; Cremonesi, P.; Warner, C. D.; Nagel, D. L.; Tomer, K. B.; Cerny, R. L.; Gross, M. L. *J. Am. Chem. Soc.* **1988**, *110*, 4023−4029.
(24) Kohda, K.; Tsunomoto, H.; Kasamatsu, T.; Sawamura, F.; Terashima, I.; Shibutani, S. *Chem. Res. Toxicol.* **1997**, *10*, 1351−1358.
(25) Akanni, A.; Abul-Hajj, Y. J. *Chem. Res. Toxicol.* **1999**, *12*, 1247−1253.

(26) Enya, T.; Kawanishi, M.; Suzuki, H.; Matsui, S.; Hisamatsu, Y. *Chem. Res. Toxicol.* **1998**, *11*, 1460−1467.
(27) Dai, J.; Wright, M. W.; Manderville, R. A. *Chem. Res. Toxicol.* **2003**, *16*, 817−821.
(28) Dai, J.; Sloat, A. L.; Wright, M. W.; Manderville, R. A. *Chem. Res. Toxicol.* **2005**, *18*, 771−779.
(29) Vaidyanathan, V. G.; Villalta, P. W.; Sturla, S. J. *Chem. Res. Toxicol.* **2007**, *20*, 913−919.
(30) Dahlmann, H. A.; Sturla, S. J. *Eur. J. Org. Chem.* **2011**, 2987−2992.
(31) Dumas, A.; Luedtke, N. W. *J. Am. Chem. Soc.* **2010**, *132*, 18004−18007.
(32) Li, C.; Hoffman, M. Z. *J. Phys. Chem. B* **1999**, *103*, 6653−6656.
(33) Hansch, C.; Leo, A.; Taft, R. W. *Chem. Rev.* **1991**, *91*, 165−195.
(34) Hammett, L. P. *Physical Organic Chemistry*; McGraw-Hill Book Co., Inc.: New York, 1940; p 206.
(35) Taft, R. W., Jr. In *Steric Effects in Organic Chemistry*; Newman, M. S., Ed.; John Wiley & Sons, Inc.: New York, 1956; p 593.
(36) Charton, M. *Can. J. Chem.* **1960**, *38*, 2493−2499.
(37) Hammett, L. P. *J. Am. Chem. Soc.* **1937**, *59*, 96−103.
(38) Oivanen, M.; Lönnberg, H.; Zhou, X.-X.; Chattopadhyaya, J. *Tetrahedron* **1987**, *43*, 1133−1140.
(39) Rankin K. M. Ph.D. Thesis, University of Guelph, Guelph, ON, December, 2012.
(40) Linnell, R. H. *J. Org. Chem.* **1960**, *25*, 290−290.
(41) Uno, B.; Iwamoto, T.; Okumura, N. *J. Org. Chem.* **1998**, *63*, 9794−9800.
(42) Greco, F.; Liguori, A.; Sindona, G.; Uccella, N. *J. Am. Chem. Soc.* **1990**, *112*, 9092−9096.
(43) Xia, F.; Xie, H.; Cao, Z. *Int. J. Quantum Chem.* **2008**, *108*, 57−65.
(44) Liu, J.; Cao, S.; Jia, B.; Wei, D.; Liao, X.; Lu, J.; Zhao, Y. *Int. J. Mass Spectrom.* **2009**, *282*, 1−5.
(45) Greisch, J.-F.; Leyh, B.; De Pauw, E. *Eur. Phys. J. D* **2009**, *51*, 89−96.
(46) Sagoo, S.; Beach, D. G.; Manderville, R. A.; Gabryelski, W. *J. Mass. Spectrom.* **2011**, *46*, 41−49.
(47) Rankin, K. M.; Sproviero, M.; Rankin, K.; Sharma, P.; Wetmore, S. D.; Manderville, R. A. *J. Org. Chem.* **2012**, *77*, 10498−10508.
(48) D'Angelo, N. D.; Peterson, J. J.; Booker, S. K.; Fellows, I.; Dominguez, C.; Hungate, R.; Reider, P. J.; Kim, T.-S. *Tetrahedron Lett.* **2006**, *47*, 5045−5048.
(49) Zhang, Q.; Wang, D.; Wang, X.; Ding, K. *J. Org. Chem.* **2009**, *74*, 7187−7190.
(50) Yong, F.-F.; Teo, Y.-C.; Yan, Y.-K.; Chua, G.-L. *Synlett* **2012**, *23*, 101−106.
(51) Fujikawa, K.; Kondo, K.; Yokomichi, I.; Kimura, F.; Haga, T.; Nishiyama, R. *Agric. Biol. Chem.* **1970**, *34*, 68−79.
(52) Chang, G.; Guida, W. C.; Still, W. C. *J. Am. Chem. Soc.* **1989**, *111*, 4379−4386.
(53) *HyperChem 8.0.8*; Hypercube, Inc.: Gainesville, FL, 2007.
(54) Frisch, M. J.; Trucks, G. W.; Schlegel, H. B.; Scuseria, G. E.; Robb, M. A.; Cheeseman, J. R.; Scalmani, G.; Barone, V.; Mennucci, B.; Petersson, G. A.; Nakatsuji, H.; Caricato, M.; Li, X.; Hratchian, H. P.; Izmaylov, A. F.; Bloino, J.; Zheng, G.; Sonnenberg, J. L.; Hada, M.; Ehara, M.; Toyota, K.; Fukuda, R.; Hasegawa, J.; Ishida, M.; Nakajima, T.; Honda, Y.; Kitao, O.; Nakai, H.; Vreven, T.; Montgomery, Jr., J. A.; Peralta, J. E.; Ogliaro, F.; Bearpark, M.; Heyd, J. J.; Brothers, E.; Kudin, K. N.; Staroverov, V. N.; Kobayashi, R.; Normand, J.; Raghavachari, K.; Rendell, A.; Burant, J. C.; Iyengar, S. S.; Tomasi, J.; Cossi, M.; Rega, N.; Millam, N. J.; Klene, M.; Knox, J. E.; Cross, J. B.; Bakken, V.; Adamo, C.; Jaramillo, J.; Gomperts, R.; Stratmann, R. E.; Yazyev, O.; Austin, A. J.; Cammi, R.; Pomelli, C.; Ochterski, J. W.; Martin, R. L.; Morokuma, K.; Zakrzewski, V. G.; Voth, G. A.; Salvador, P.; Dannenberg, J. J.; Dapprich, S.; Daniels, A. D.; Farkas, Ö.; Foresman, J. B.; Ortiz, J. V.; Cioslowski, J.; Fox, D. J. *Gaussian 09*, Revision A.02; Gaussian, Inc.: Wallingford, CT, 2009.
(55) Frisch, M. J.; Trucks, G. W.; Schlegel, H. B.; Scuseria, G. E.; Robb, M. A.; Cheeseman, J. R.; Scalmani, G.; Barone, V.; Mennucci, B.; Petersson, G. A.; Nakatsuji, H.; Caricato, M.; Li, X.; Hratchian, H. P.; Izmaylov, A. F.; Bloino, J.; Zheng, G.; Sonnenberg, J. L.; Hada, M.; Ehara, M.; Toyota, K.; Fukuda, R.; Hasegawa, J.; Ishida, M.; Nakajima, T.; Honda, Y.; Kitao, O.; Nakai, H.; Vreven, T.; Montgomery, J. A., Jr.; Peralta, J. E.; Ogliaro, F.; Bearpark, M.; Heyd, J. J.; Brothers, E.; Kudin, K. N.; Staroverov, V. N.; Keith, T.; Kobayashi, R.; Normand, J.; Raghavachari, K.; Rendell, A.; Burant, J. C.; Iyengar, S. S.; Tomasi, J.; Cossi, M.; Rega, N.; Millam, J. M.; Klene, M.; Knox, J. E.; Cross, J. B.; Bakken, V.; Adamo, C.; Jaramillo, J.; Gomperts, R.; Stratmann, R. E.; Yazyev, O.; Austin, A. J.; Cammi, R.; Pomelli, C.; Ochterski, J. W.; Martin, R. L.; Morokuma, K.; Zakrzewski, V. G.; Voth, G. A.; Salvador, P.; Dannenberg, J. J.; Dapprich, S.; Daniels, A. D.; Farkas, O.; Foresman, J. B.; Ortiz, J. V.; Cioslowski, J.; Fox, D. J. *Gaussian 09*, Revision C.01; Gaussian, Inc.: Wallingford, CT, 2010.